JACS
JOURNAL OF THE AMERICAN CHEMICAL SOCIETY

ARTICLE

pubs.acs.org/JACS

Structure of the Borosilicate Zeolite Catalyst SSZ-82 Solved Using 2D-XPD Charge Flipping

Dan Xie, Lynne B. McCusker,* and Christian Baerlocher

Laboratory of Crystallography, ETH Zurich, CH-8093 Zurich, Switzerland

Supporting Information

ABSTRACT: The structure of the calcined borosilicate zeolite catalyst SSZ-82 ($[Si_{61.3}B_{4.7}O_{132}]$, *Pmmn*, a = 24.2783(4), b = 11.4665(2), and c = 14.1127(3) Å) has been solved from X-ray powder diffraction (XPD) data using the recently developed 2D-XPD charge flipping approach. The electron density maps generated with the more conventional powder charge flipping (pCF) algorithm could not be interpreted easily, so this new method, which begins by phasing low-resolution, 2D subsets of the data, was applied. Crystallographic phases were derived for the three main projections ([100], [010], and [001]) by using just the corresponding subsets of reflections (0*kl*, *h*0*l*, and *hk*0, respectively) from the full set of 3039 extracted intensities. These phases were then imposed on the (otherwise random) starting phases in the application of the pCF algorithm to the full data set. The framework structure, with 11 Si/B atoms in the asymmetric unit and a novel 12-/10-ring 2D channel system, could be seen clearly in the resulting electron density map. This is the first application of the 2D-XPD method to data collected on a material of unknown structure. Rietveld refinement of the structure revealed the positions of the B atoms in the framework and indicated that some water had been readsorbed in the pores.

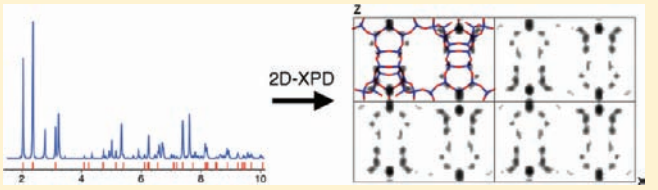

1. INTRODUCTION

The properties of zeolites (e.g., ion exchange, adsorption, shape selectivity or catalytic activity) are essentially determined by their structures. This is why considerable effort is put into synthesizing new zeolites with different framework architectures: Their properties are likely to be novel or perhaps particularly well-suited for a specific application. The zeolite SSZ-57, whose extremely complex framework structure was recently elucidated,[1] was built upon a synthesis strategy developed by Elomari using enamine chemistry.[2] Cyclic ketones are reacted with cyclic amines, like pyrrolidine, reduced, and then a fourth group is added to the nitrogen to make a charged structure-directing agent (SDA). For SSZ-57, the SDA was the bulky *N*-butyl-*N*-cyclohexyl-pyrrolidinium cation. When the even larger SDA, *N*-butyl-*N*-cyclooctylpyrrolidinium, was used, the zeolite SSZ-58, with unique double five-ring composite building units (CBU), was produced.[3] In another study, Zones and co-workers explored the use of heterocyclic molecules at each end of methyene chains of different lengths to develop diquaternary SDAs.[4] One of the surprising results of that investigation was the discovery of the zeolite SSZ-74, with an ordered Si vacancy in its framework structure.[5] In the course of an investigation combining these two concepts, enamine chemistry and diquaternary SDAs, Burton synthesized the borosilicate zeolite SSZ-82,[6] which is the subject of the present study.

At the time, the prospect of the structure having both 10- and 12-ring pores was considered possible, because single-crystal structure analysis of the zeolite SSZ-35, which was synthesized with a related SDA, showed that the SDA bridged from one cavity to the next via a 10-ring window.[7] Zeolites with both 10- and 12-ring channels have emerged as valuable catalysts because of their impressive catalytic activity and stability, often comparing favorably with the commerically available multidimensional large-pore high-silica zeolite beta.[8,9] Therefore, there was considerable interest in learning the details of the structure of this novel zeolite. Empirical tests had already shown it to be an active and stable catalyst.[6]

Unfortunately, like most newly synthesized zeolites, the samples of SSZ-82 are polycrystalline, so the structure analysis had to be performed using X-ray powder diffraction (XPD) data. Although this is more difficult than solving the structure from single-crystal data, powder diffraction methodology has developed enormously over the last 20 years,[10] and now a moderately complex structure can usually be solved in a relatively straightforward manner. Structure solution in general can be described as a process by which the correct crystallographic phases for all reflections in a data set are determined. From the measured intensities and these phases, an electron density map can be generated, and the atoms in the structure located. The trick is in arriving at the correct phases.

The powder charge flipping (pCF) algorithm[11] in the computer program Superflip[12] has been shown to be a powerful one for solving this phase problem even with powder diffraction data, where many of the reflection intensities are ambiguous.[13] In the case of more complex structures, such as those of the zeolites IM-5,[14] SSZ-74,[5] and ITQ-37,[15] it has been shown that including additional information derived from electron microscopy techniques

Received: September 30, 2011
Published: November 11, 2011

Table 1. XPD Data Collection

synchrotron facility	SNBL (Station B) at ESRF
wavelength	0.50117 Å
diffraction geometry	Debye−Scherrer
analyzer crystal	Si 1 1 1
sample	rotating 1.0 mm capillary
2θ range	1−33°
step size	0.003°2θ
time per step	
1.0−3.6°2θ	1.7 s
3.6−8.4°2θ	3.7 s
8.4−11.6°2θ	6.2 s
11.6−33.0°2θ	9.7 s

(high-resolution transmission electron microscopy (HRTEM) images or selected area electron diffraction data) in the procedure made the difference between solving and not solving the structure. However, it is not always easy to obtain electron microscopy data, especially for beam-sensitive materials like zeolites. Therefore, we have developed an alternative approach for difficult cases, which we have dubbed 2D-XPD.[16]

The 2D-XPD method evolved from the successful combination of high-resolution powder diffraction intensities with phases derived from 2D precession electron diffraction (PED) data.[17] Including just these few phases from PED patterns in the (otherwise random) starting phase set in Superflip proved to be extremely effective. It was reasoned that if reliable phases could be derived from the imperfect PED intensities, perhaps the same would be true for imperfect XPD intensities. The reasons for the inaccuracies in the reflection intensities are different (PED data suffer from multiple scattering and XPD data from reflection overlap), but the magnitudes of the errors are comparable. Indeed, tests on the three most complex zeolite structures known, TNU-9,[18] IM-5,[14] and SSZ-74,[5] showed that the method worked. With this 2D-XPD approach, all three structures, which could only be solved originally by combining XPD and electron microscopy data, could be solved using XPD data alone.

Preliminary evaluation of the powder diffraction data for SSZ-82 indicated that the structure would be moderately complex. The unit cell is quite large (a = 24.28, b = 11.47, and c = 14.11 Å; V = 3930 Å^3), and as a result of the fact that $a \sim \sqrt{3}c$, the reflection overlap is particularly high (89% of the reflections are within 0.25*full width at half-maximum (fwhm) of a neighboring one). From the size of the unit cell and its symmetry, at least 8 Si/B atoms in the asymmetric unit were expected. Initial attempts to solve the structure directly using the normal powder charge flipping algorithm were not successful, so it appeared to be an ideal test case for the 2D-XPD procedure.

2. EXPERIMENTAL SECTION

The sample of SSZ-82 used for this study was synthesized by Allen Burton[6] and kindly provided by Stacey Zones, Chevron Energy and Technology Co. Chemical analysis yielded a Si:B ratio of 35.7:1. The sample was calcined in air at 595 °C for 5 h and then packed into a 1 mm glass capillary and sealed. High-resolution XPD data were collected on the Swiss−Norwegian Beamline (SNBL) at the European Synchrotron Radiation Facility (ESRF) in Grenoble, France. Because the data collection was done several months after the capillary had been filled, it is possible that some rehydration occurred. More details of the data collection are given in Table 1.

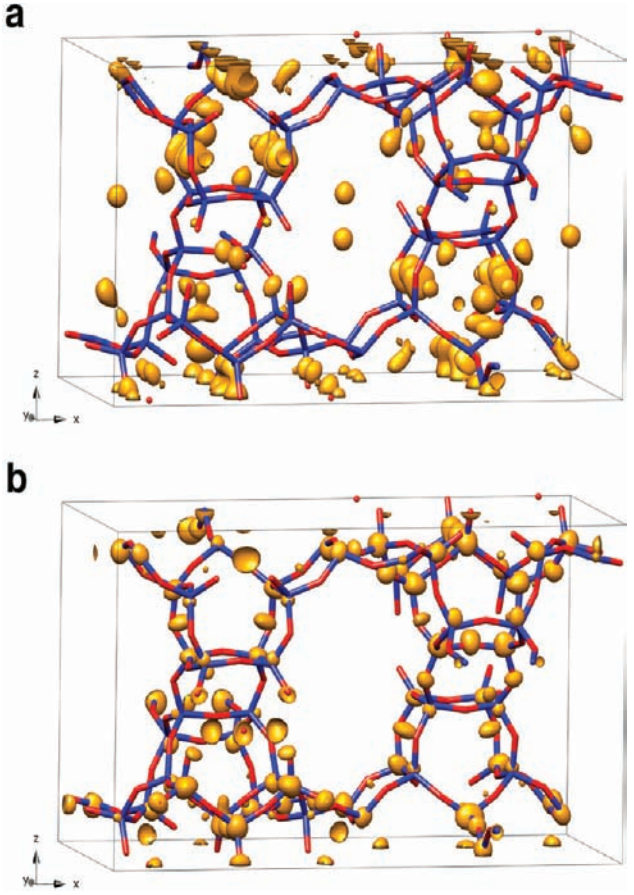

Figure 1. Electron density maps for SSZ-82 obtained using (a) the conventional powder charge flipping algorithm and (b) the 2D-XPD charge flipping approach. A stick model of the refined structure has been superimposed for comparison (blue: Si; red: O).

3. RESULTS

Structure Solution. The diffraction pattern could be indexed with a primitive orthorhombic unit cell (a = 24.2934, b = 11.4811, and c = 14.1186 Å) using the program TREOR[19] implemented in the software CMPR.[20] A careful examination of the diffraction pattern indicated that $hk0$ reflections with $h + k = 2n + 1$ were systematically absent, so the most probable space groups were expected to be centrosymmetric $Pmmn$ or one of its noncentrosymmetric subgroups $Pm2_1n$ or $P2_1mn$.

Individual reflection intensities were extracted from the powder pattern to a minimum d-spacing of 0.90 Å (ca. 32.5°2θ), assuming the space group $Pmmn$ and using the program EXTRACT[21] in the XRS-82 suite of programs.[22] These intensities were used as input to the pCF algorithm in Superflip for structure solution. An approximate chemical composition of $Si_{64}O_{128}$ per unit cell was assumed for the histogram matching procedure that is coupled to the repartitioning of overlapping reflections during the course of the pCF iterations. Reflections within 0.25*fwhm of one another were defined as overlapping. Of the 3039 reflections, 2706 are overlapping (89.1%), and they fall into 396 overlap groups.

Initially, no symmetry was imposed during the pCF runs because the space group was not clear. However, the $P1$ electron density maps generated by Superflip were not satisfactory. Imposing the symmetry (assuming $Pmmn$) improved the quality

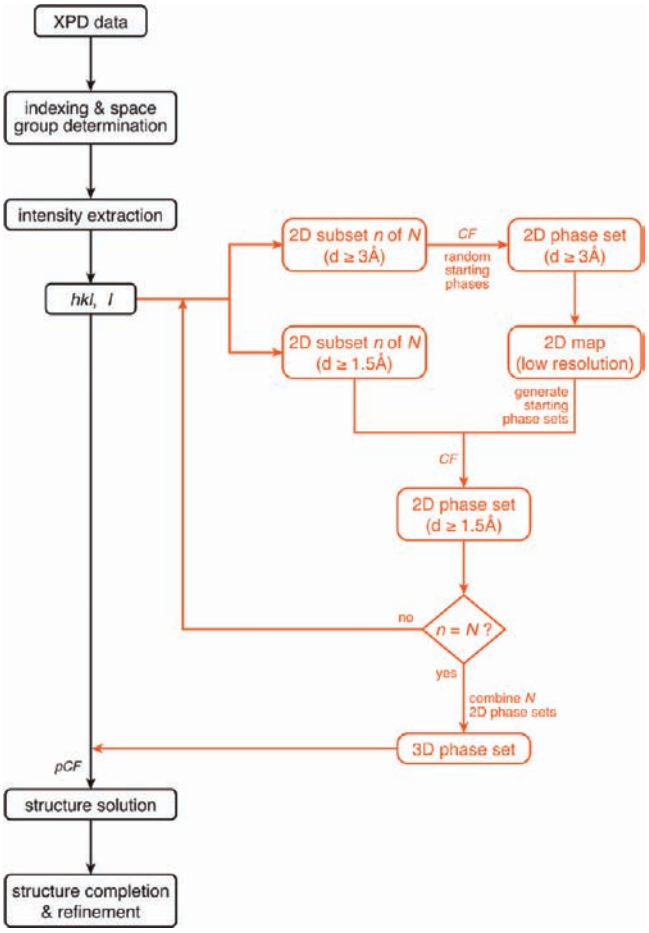

Figure 2. Flowchart of the 2D-XPD powder charge-flipping method (highlighted in orange).

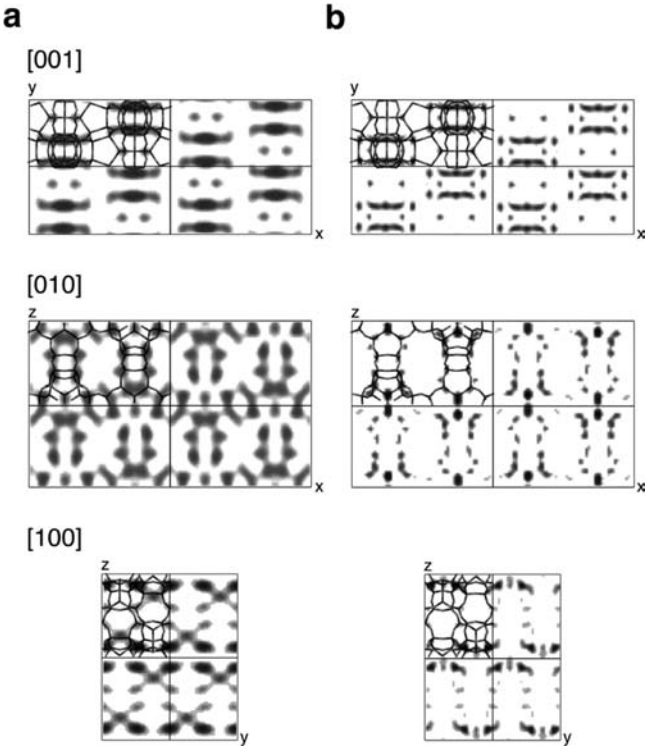

Figure 3. Two-dimensional projections (2 × 2 cells) of the electron density of SSZ-82 along the [001], [010], and [100] directions generated from (a) 3 and (b) 1.5 Å resolution XPD amplitudes and 2D-XPD phases. For each map, the corresponding projection of the framework structure has been superimposed in one unit cell for comparison.

of the maps slightly (the electron density peaks became more spherical), but it was still not possible to derive the structure from the maps (Figure 1a). Therefore, the 2D-XPD approach[16] was tried. The procedure (Figure 2) used can be described as follows: (1) The subset of reflections corresponding to each of the projections of interest ([001], [010], and [100] in this case) was selected from the full set of extracted reflection intensities. (2) For each projection, just those reflections with $d \geq 3.0$ Å were used as input to the single-crystal charge-flipping (CF) routine in Superflip (100 runs of 300 cycles, flipping threshold value δ = 0).[23] (3) For each projection, the 40 best phase sets in the second step were selected and subjected to a cluster analysis.[24] The cluster of phase sets found to be most similar was averaged, and the corresponding electron density map calculated (Figure 3a). This map was then used as a starting point (100 new starting phase sets generated from the map by allowing the phases to vary by up to 30% in a random fashion) for a second Superflip run with 1.5 Å data (Figure 3b). (4) The three projections were shifted to a common origin by matching the phases of common reflections to generate a consistent set of phases for 218 reflections. (5) These phases were imposed on the starting phase sets for pCF runs using the full 3D data set.

A posteriori analysis showed the amplitude-weighted phase correctness for the three projections [001], [010], and [100] for SSZ-82 to be 77, 74, and 86%, respectively. That is, the retrieved phases were quite good, even though the amplitudes used to derive them were inaccurate because of reflection overlap. In each projection, more than half of the reflections overlap with other reflections of the full 3D data set.

Table 2. Powder Charge Flipping Input Parameters[a]

input phases enforced for	first 50 cycles
chemical composition assumed for HM	$Si_{64}O_{128}$
first HM	after 50 cycles
subsequent HM	every 10 cycles
overlap factor (fwhm)	0.25
d_{min} (Å)	0.91
flipping threshold value δ	determined by Superflip
runs	100
cycles per run	500

[a] HM: histogram matching; fwhm: full width at half-maximum.

Further details of the Superflip run are given in Table 2. With the inclusion of the 2D-XPD starting phases, the solution was much more reasonable than the one obtained with random starting phases. A very clear framework structure was achieved by applying a second series of pCF runs using the previous solution as a seed to generate new starting phase sets (Figure 1b).

Structure Refinement. The geometry of the framework structure model derived from the 2D-XPD charge-flipping runs was optimized using the program DLS-76[25] and then used as a starting point for Rietveld refinement. In view of the chemical analysis, all 11 symmetry independent T atoms were refined

Table 3. Crystallographic Data for SSZ-82

chemical composition (from refinement)	$\|(H_2O)_{15.7}\|[Si_{61.3}B_{4.7}O_{132}]$
unit cell	
a	24.2783(4) Å
b	11.4665(2) Å
c	14.1127(3) Å
space group	*Pmmn*
number of observations	6275
number of contributing reflections	3039
number of geometric restraints	116
number of structural parameters	99
number of profile parameters	10
R_F	0.040
R_{wp}	0.140
R_{exp}	0.129

selected bond distances (Å) and angles (°)[a]		min	max	avg
Si−O	(1.61 Å)	1.58	1.62	1.60
(Si,B)−O	(1.57, 1.58 Å)	1.57	1.62	1.59
O−Si−O	(109.5)	103.0	113.6	109.4
O−(Si,B)−O	(109.5)	103.2	114.0	109.4
Si−O−Si	(145)	141.8	175.3	155.1
Si−O−(Si,B)	(145)	138.7	145.0	141.6
(Si,B)−O−(Si(B)	(145)	134.5	168.6	152.3

[a] Prescribed values used for the restraints are given in parentheses.

initially as Si atoms with full occupancies. Geometric restraints were placed on the bond distances and angles of the framework atoms, and their positions refined. These restraints were imposed throughout the refinement (see Table 3), but their relative weighting with respect to the powder diffraction data was reduced as the refinement progressed. From a series of difference Fourier maps, four nonframework atom positions were identified. Inclusion of these as water molecules with partial occupancies reduced the R_{wp} value from 0.418 to 0.239.

Once the nonframework electron density had been described, the positions of the framework atoms were refined to convergence, and then the occupancies of the Si-atom positions were allowed to vary. The occupancies of two T-sites (Si(10) and Si(11), see Supporting Information) refined to values significantly less than 1.0, so it was assumed that these were partially occupied with B. The other nine T-sites appeared to be pure Si. This result is consistent with the fact that previous difference Fourier maps had also shown negative differences at these two Si positions. Therefore, B was added at each of these positions with an initial occupancy of 0.10 and a constraint that the total occupancy (Si + B) be 1.0 at each position. Eventually, the occupancy of Si(10) refined to 0.75 (B(10) 0.25) and that of Si(11) to 0.66 (B(11) 0.34). This reduced the R_{wp} value from 0.150 to 0.140 and the R_F value from 0.044 to 0.040. The amount of B is significantly different from that found by chemical analysis, but such differences have also been observed in other borosilicates. The Si/B-distance restraints were adjusted to reflect the presence of B, and this resulted in a slightly improved geometry.

In the final model, there are 4 water positions in the channels in addition to the 9 Si, 2 mixed Si/B, and 23 O atom positions describing the framework structure. It appears that the sample was no longer completely dehydrated when the data were collected. For the refinement, the displacement parameters for these water molecules were fixed arbitrarily at $U_{iso} = 0.08$, and the positions and occupancies refined. While these atoms refined to chemically sensible positions making good H-bonding contacts with one another, they should not be overinterpreted. They simply describe an ill-defined cloud of electron density in the channels. The occupancies refined to a total of 15.7 water molecules per unit cell. Refinement of this structural model converged with $R_F = 0.040$ and $R_{wp} = 0.140$ ($R_{exp} = 0.129$). The highest peak on the final difference electron density map was 0.5 e/Å^3 and the lowest −0.5 e/Å^3. All atoms were refined isotropically using scattering factors for neutral atoms. The displacement parameters for similar atoms were constrained to be equal to keep the number of parameters to a minimum. Details of the refinement and selected bond distances and angles are given in Table 3, a cif file with the final atomic parameters is provided in the Supporting Information, and the fit of the profile calculated from the final model to the experimental data is shown in Figure 4.

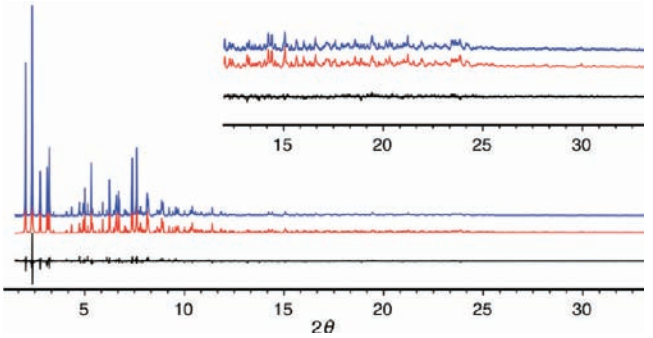

Figure 4. Observed (top), calculated (middle), and difference (bottom) profiles for the Rietveld refinement of SSZ-82. The profiles in the inset have been scaled up by a factor of 5 to show more detail. Tick marks indicate the positions of the reflections.

4. DISCUSSION

The framework structure of SSZ-82 can be described as an ordered arrangement of building blocks consisting of 2 *lau*, 1 *afs*, and 1 *bea* composite building units.[26] These building blocks (Figures 5a and b) repeat along the *z*-direction (Figure 5c) and are linked via 5-rings along the *y* direction to form 10-rings (4.9 × 5.5 Å) (Figure 5d). Along the *x* direction, the building blocks are arranged in an up−down fashion and are displaced by $y = 1/2$. These columns are connected directly to one another to form 4-rings and elliptical 12-ring (5.2 × 8.0 Å) channels along the *y* direction (Figure 5e). Because of the $y = 1/2$ displacement of the columns, the 10-rings form a zigzag channel along the *x* direction and intersect with the straight 12-ring channels along the *y* direction (Figure 5f) to form a 2D 10-/12-ring channel system (Figure 5g, 6).

Only three other zeolites, the borosilicate SSZ-56 (**SFS**),[27] the rare aluminosilicate mineral boggsite (**BOG**),[28] and the cobalto-gallophosphate IM-6 (**USI**)[29] are known to have such channel systems. Simancas et al. recently reported the targeted synthesis of the **BOG** framework type in a borosilicate system (ITQ-47).[30] It is interesting to note that with SSZ-82, 3 of the 4 framework types with 2D 10-/12-ring channel systems have been synthesized in borosilicate systems. The combination of intersecting large and medium sized channels is of interest for catalytic applications. Their different sorption, diffusion, and catalytic properties were analyzed some years ago by Corma.[31] The 10-/12-ring

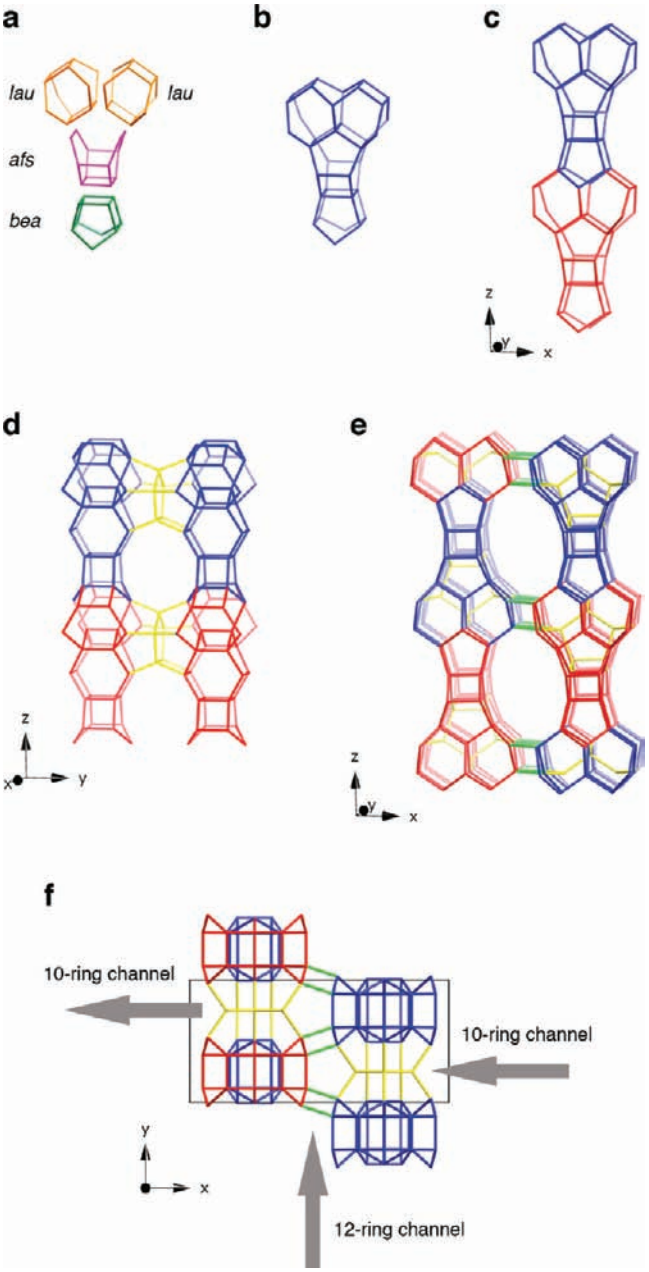

Figure 5. The construction of the framework structure SSZ-82. (a) The *lau*, *afs*, and *bea* CBUs assembled to form (b) a repeating building block. (c) The arrangement of the building blocks in (b) along the *z* direction. (d) The connection of the columns in (c) along the *y* direction to form 10-rings. (e) The connection of the layers in (d) along the *x* direction to form 12-ring channels. (f) The [001] projection showing the arrangement of the 10- and 12-ring channels.

channel intersections for **SFS**, **BOG**, **USI**, and SSZ-82 are quite different and are shown for comparison in Figure 7.

In the SSZ-82 framework structure, the distribution of B atoms was determined from the Rietveld refinement. The two mixed Si/B sites (Si/B(10) and Si/B(11)) form the three 4-rings at the base of the *afs* CBU (Figure 8). They are thus located in the 4-rings that separate neighboring 12-rings along the *x* direction. The water molecules at Ow(1) and Ow(3) are located in the 12-ring channel, and those at Ow(2) in the 10-ring channel and those at Ow(4) are close to the intersection of the 12- and 10-ring

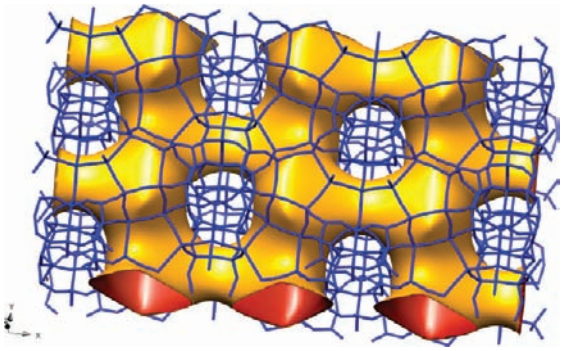

Figure 6. A structure envelope[32] (yellow) highlighting the 12-/10-ring 2D channel system in the SSZ-82 framework structure (blue).

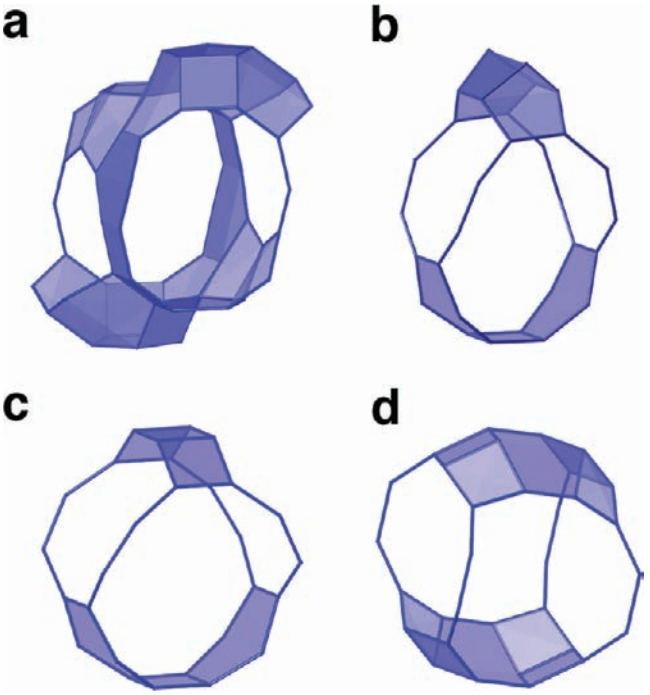

Figure 7. The 10-/12-ring channel intersections for (a) SSZ-82, (b) **SFS**, (c) **BOG**, and (d) **USI**. Bridging O atoms have been omitted for clarity.

channels (Figure 8). All water positions are at least 3.5 Å away from framework atoms, but they do form a hydrogen-bonded network among themselves.

This ab initio determination of the structure of SSZ-82 from powder diffraction data provides a clear demonstration of the power of the 2D-XPD powder charge-flipping approach. Although most of the reflection intensities derived from the powder diffraction pattern were ambiguous because of reflection overlap (89%), they could still be used to retrieve reliable low-resolution phases in two dimensions. By imposing these few phases on the initial phase set for the 3D structure solution, interpretable maps could be generated. This was not the case when the default mode of the pCF algorithm, starting with random phases, was used. The advantages of this 2D-XPD approach are two-fold: (1) only XPD data are required, so the more complicated electron microscopy experiments, whether HRTEM or PED, are not necessary, and (2) the projections used for phase retrieval can be selected

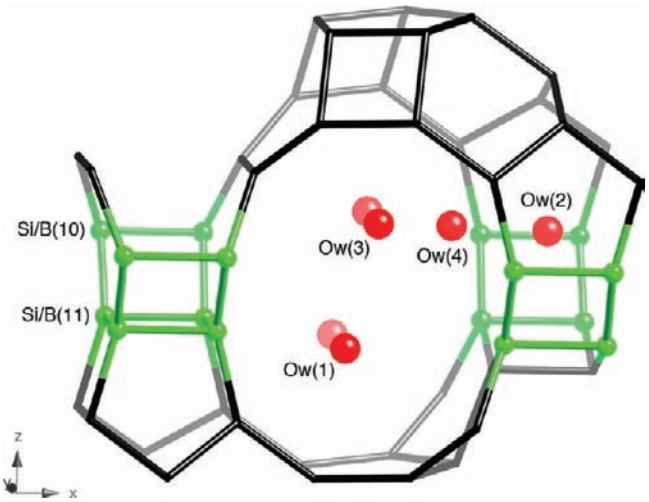

Figure 8. Location of the mixed Si/B atom positions (green) and water molecules (red) in the structure of SSZ-82. Bridging O atoms have been omitted for clarity.

arbitrarily. That is, a crystallite with the appropriate orientation and suitable thickness does not have to be found as it does for EM experiments. This 2D-XPD approach has the further advantage that it is general and can be applied to data collected on any polycrystalline material. No prior chemical knowledge other than the chemical composition (for histogram matching) is required.

The 2D maps shown in Figure 3 illustrate that this 2D-XPD approach can also be used to generate 2D images that are of similar or even higher quality than good HRTEM images. That is, the gross features of a structure, such as a zeolite's pore system (e.g., Figure 3b), can be visualized from such projections, even if the framework structure has not yet been solved in detail.

5. CONCLUSIONS

The structure of the novel borosilicate zeolite SSZ-82 ($[Si_{61.3}B_{4.7}O_{132}]$) has been determined from powder diffraction data using 2D-XPD powder charge flipping. This approach offers a remarkably simple and powerful method for solving the structures of complex polycrystalline materials from XPD data. The framework that emerged has 11 T-atoms in the asymmetric unit and a novel 12-/10- ring 2D channel system with effective pore widths of 5.2 × 8.0 Å and 4.9 × 5.5 Å, respectively.

■ ASSOCIATED CONTENT

Supporting Information. Crystallographic information file for SSZ-82 (CIF). This material is available free of charge via the Internet at http://pubs.acs.org.

■ AUTHOR INFORMATION

Corresponding Author
mccusker@mat.ethz.ch.

■ ACKNOWLEDGMENT

We thank the beamline scientists at the SNBL at the ESRF in Grenoble, France, for their assistance with the powder diffraction measurements, and Stacey Zones for useful discussions regarding the synthesis and applications of the SSZ-82 material. Financial support for D.X. was provided by the Chevron Energy and Technology Company.

■ REFERENCES

(1) Baerlocher, Ch.; Weber, T.; McCusker, L. B.; Palatinus, L.; Zones, S. I. *Science* **2011**, *333*, 1134.
(2) Elomari, S. Process for preparing zeolites using pyrrolidinium cations. U.S. Patent 6,616,911, 2003.
(3) (a) Elomari, S. Zeolite SSZ-58 composition of matter and synthesis thereof. U.S. Patent 6,555,089, 2003. (b) Burton, A. W.; Elomari, S.; Medrud, R. C.; Chan, I. Y.; Chen, C.-Y.; Bull, L. M.; Vittoratos, E. *J. Am. Chem. Soc.* **2003**, *125*, 1633.
(4) Jackowski, A.; Zones, S. I.; Hwang, S.-J.; Burton, A. W. *J. Am. Chem. Soc.* **2009**, *131*, 1092.
(5) Baerlocher, Ch.; Xie, D.; McCusker, L. B.; Hwang, S.-J.; Chan, I. Y.; Ong, K.; Burton, A. W.; Zones, S. I. *Nat. Mater.* **2008**, *7*, 631.
(6) Burton, A. W. Molecular sieve SSZ-82 composition of matter and synthesis thereof. U.S. Patent 7,820,141, 2010.
(7) Zones, S. I.; Hwang, S.-J.; Olmstead, M. M.; Teat, S. J.; Jackowski, A.; Burton, A. W.; Kim, C. *J. Phys. Chem. C* **2010**, *114*, 8899.
(8) Gil, B.; Zones, S. I.; Hwang, S.-J.; Bejblova, M.; Cejka, J. *J. Phys. Chem. C* **2008**, *112*, 2997.
(9) Moliner, M.; Gonzolez, J.; Portilla, M. T.; Willhammar, T.; Rey, F.; Llopis, F. J.; Zou, X.; Corma, A. *J. Am. Chem. Soc.* **2011**, *133*, 9497.
(10) David, W. I. F.; Shankland, K. *Acta Crystallogr., Sect. A: Cryst. Phys., Diffr., Theor. Gen. Crystallogr.* **2008**, *64*, 52 and references therein.
(11) Baerlocher, Ch.; McCusker, L. B.; Palatinus, L. *Z. Kristallogr.* **2007**, *222*, 47.
(12) Palatinus, L.; Chapuis, G. *J. Appl. Crystallogr.* **2007**, *40*, 786.
(13) (a) Koyama, Y.; Ikeda, T.; Tatsumi, T.; Kubota, Y. *Angew. Chem., Int. Ed.* **2008**, *47*, 1042. (b) Xie, D.; McCusker, L. B.; Baerlocher, Ch.; Gibson, L.; Burton, A. W.; Hwang, S. J. *J. Phys. Chem. C.* **2009**, *113*, 9845. (c) Palatinus, L.; Damay, F. *Acta Crystallogr., Sect. B: Struct. Sci.* **2009**, *65*, 784. (d) Sisak, D.; McCusker, L. B.; Zandomeneghi, G.; Meier, B. H.; Blaser, D.; Boese, R.; Schweizer, W. B.; Gilmour, R.; Dunitz, J. D. *Angew. Chem., Int. Ed.* **2010**, *49*, 4503. (e) Park, M. B.; Hong, S. B.; Cho, S. J. *J. Am. Chem. Soc.* **2011**, *133*, 1917. (f) Liu, L.; Yang, J.; Li, J.; Dong, J.; Sisak, D.; Luzzatto, M.; McCusker, L. B. *Angew. Chem., Int. Ed.* **2011**, *50*, 8139.
(14) Baerlocher, Ch.; Gramm, F.; Massueger, L.; McCusker, L. B.; He, Z. B.; Hovmoller, S.; Zou, X. D. *Science* **2007**, *315*, 1113.
(15) Sun, J. L.; Bonneau, C.; Cantín, A.; Corma, A.; Díaz-Cabanas, M. J.; Moliner, M.; Zhang, D.; Li, M.; Zou, X. D. *Nature* **2009**, *458*, 1154.
(16) Xie, D.; Baerlocher, Ch; McCusker, L. B. *J. Appl. Crystallogr.* **2011**, *44*, 1023.
(17) Xie, D.; Baerlocher, Ch; McCusker, L. B. *J. Appl. Crystallogr.* **2008**, *41*, 1115.
(18) Gramm, F.; Baerlocher, Ch.; McCusker, L. B.; Warrender, S. J.; Wright, P. A.; Han, B.; Hong, S. B.; Liu, Z.; Ohsuna, T.; Terasaki, O. *Nature* **2006**, *444*, 79.
(19) Werner, P. E.; Eriksson, L.; Westdahl, M. *J. Appl. Crystallogr.* **1985**, *18*, 367.
(20) Toby, B. H. *J. Appl. Crystallogr.* **2005**, *38*, 1040.
(21) Baerlocher, Ch. *EXTRACT. A Fortran program for the extraction of integrated intensities from a powder pattern*; Institut für Kristallographie, ETH: Zürich, Switzerland, 1990.
(22) Baerlocher, Ch.; Hepp, A. *XRS-82. The X-ray Rietveld System*; Institut für Kristallographie, ETH : Zürich, Switzerland, 1982.
(23) Previous tests on known structures have shown that the quality of 2D maps improves significantly if the key parameter in the charge-flipping algorithm, the flipping threshold value δ, is set to zero and not determined automatically by the program Superflip.
(24) The statistical cluster analysis procedure was performed using the program Cluster 3.0 [see (a)]; the "Euclidean distance" metric and the "average linkage" method were chosen for the calculation. The clustering results were viewed using the program Java TreeView [see

(b)]. (a) de Hoon, M. J. L.; Imoto, S.; Nolan, J.; Miyano, S. *Bioinformatics.* **2004**, *20*, 1453. (b) Saldanha, A. J. *Bioinformatics* **2004**, *20*, 3246.
(25) Baerlocher, Ch.; Hepp, A.; Meier, W. M. *DLS-76*; Institut für Kristallographie, ETH: Zürich, Switzerland, 1976.
(26) Baerlocher, Ch.; McCusker, L. B; Olson, D. H. *Atlas of Zeolite Framework Types*, 6th revised ed.; Elsevier: Amsterdam, The Netherlands, 2007.
(27) (a) Elomari, S.; Burton, A.; Medrud, R. C.; Grosse-Kunstleve, R. *Microporous Mesoporous Mat.* **2009**, *118*, 325.(b) Elomari, S. Hydrocarbon conversion using molecular sieve SSZ-56. U.S. Patent 7,390,395B2, 2008.
(28) Pluth, J. J.; Smith, J. V. *Am. Mineral.* **1990**, *75*, 501.
(29) Josien, L.; Simon Masseron, A.; Gramlich, V.; Patarin, J.; Rouleau, L. *Chem.—Eur. J.* **2003**, *9*, 856.
(30) Simancas, R.; Dari, D.; Velamazan, N.; Navarro, M. T.; Cantin, A.; Jorda, J. L.; Sastre, G.; Corma, A.; Rey, F. *Science* **2010**, *330*, 1219.
(31) Corma, A. *Microporous Mesoporous Mater.* **1998**, *21*, 487.
(32) Brenner, S.; McCusker, L. B.; Baerlocher, C. *J. Appl. Crystallogr.* **1997**, *30*, 1167.